Supporting Information

Suzuki et al. 10.1073/pnas.1423520112

SI Materials and Methods

Construction of AviTagged HABD. For the biotinylation of CD44 HABD, the AviTag peptide sequence (GLNDIFEAQKIEWHE) was attached at either the C terminus or the N terminus of HABD. For the C-terminal AviTagged constructs, the cDNA fragment encoding the human CD44 HABD (residues Q21–V178), a flexible linker (SLLGG), and the AviTag was cloned into the pET42b vector, using the NdeI/XhoI sites. For the N-terminal AviTag construct, the cDNA fragment encoding the AviTag, a spacer sequence (GAPG), and the human CD44 HABD (residues Q21–V178) was cloned into the pET11a vector, using the NdeI/BamHI sites.

Characterization of AviTagged HABD. The heteronuclear single quantum coherence (HSQC) spectra [0.4–0.9 mM protein concentrations in 50 mM NaPi (pH 6.8), 150 mM NaCl, 10% D_2O] were recorded with Bruker Avance 500-MHz or 600-MHz spectrometers equipped with a cryogenic probe at 25 °C. Surface plasmon resonance (SPR) experiments were performed using a BIAcore T200 (GE Healthcare).

Preparation of the HABD-Coated Beads. The biotin ligase BirA was prepared, to conjugate biotin to the amino group of the lysine residue within the AviTag. Competent bacterial competent cells containing the plasmid expressing BirA (Avidity) were cultured in LB medium and induced by isopropyl-β-D-thiogalactopyranoside at 37 °C overnight. The cells were harvested by centrifugation, and BirA was purified as described previously (1). The purified BirA was then used to ligate biotin to the tag by an incubation with HABD at room temperature overnight, in a buffer containing 10 mM $MgCl_2$, 10 mM ATP, and 50 μM biotin. The biotinylated HABD was attached to avidin-coated beads (Bangs Laboratory). The amount of HABD immobilized on the beads was quantified by either a Western blot analysis using a mouse anti-biotin antibody (Jackson) or an HRP-labeled goat anti-mouse IgG antibody (R&D systems) or a flow cytometry analysis using a rat anti-CD44 antibody, IM7, and an FITC-labeled secondary antibody (Zymed).

Rolling Experiment. Polystyrene plates (35 × 10 mm; Corning) were coated with 100 μg/mL of HA oligomers in PBS, at 4 °C overnight. The plates were assembled as the lower wall in a parallel plate laminar flow chamber with the gasket thickness of 0.01 inch and the flow path width of 0.25 cm (GlycoTech) and were mounted on an ECLIPSE Ti-U inverted microscope (Nikon). The HABD-coated beads were suspended at a density of 4×10^4/mL, in PBS containing 0.1% (wt/vol) BSA and 1 mM EDTA, and were perfused over the flow chamber at 0.3 dyn/cm^2 for 5 min. In the detachment assays, the shear stress was increased every 10 s up to 2.0 dyn/cm^2. Images of the beads were recorded at 25 frames per second with a CCD camera (C9300; Hamamatsu Photonics K.K.) attached to the microscope. The data obtained from the rolling experiments were analyzed by the particle-tracking module of the ImageJ software (2).

Steered Molecular Dynamics Simulations. The steered molecular dynamics (SMD) simulations were performed with the program NAMD2 (3), using the CHARMM force fields (4). The crystal structure of the mouse CD44 HABD in complex with an HA 8mer (PDB code: 2JCR) (5) was used as the initial structure. The starting structure was solvated in a 62 × 129 × 69-Å TIP3 water box (6) with 54 chloride ions to neutralize the system, resulting in 53,872 atoms. The system was minimized for three consecutive 500-conjugate gradient steps, during which the protein was first held fixed; next, only the heavy atoms of the protein were held fixed, and finally, all atoms were allowed to move. After the energy minimizations, the system was heated gradually from 0 K to 310 K over 52 ps, and the temperature was maintained using Langevin dynamics. The pressure was maintained at 1 atom by the Langevin piston method. In SMD, the C2 atom of *N*-acetylglucosamine residue 1,177 was kept fixed, whereas the Cα atom of the mouse HABD C-terminal residue Ile-173 was pulled at a constant speed of 10 Å/ns with a spring constant of 1 kcal·mol^{-1}·Å^{-2}. The simulation was performed during a 4-ns period. Visualization and analysis of the trajectories were conducted with visual molecular dynamics (7).

1. Buoncristiani MR, Otsuka AJ (1988) Overproduction and rapid purification of the biotin operon repressor from Escherichia coli. *J Biol Chem* 263(2):1013–1016.
2. Schneider CA, Rasband WS, Eliceiri KW (2012) NIH Image to ImageJ: 25 years of image analysis. *Nat Methods* 9(7):671–675.
3. Phillips JC, et al. (2005) Scalable molecular dynamics with NAMD. *J Comput Chem* 26(16):1781–1802.
4. Brooks BR, et al. (2009) CHARMM: The biomolecular simulation program. *J Comput Chem* 30(10):1545–1614.
5. Banerji S, et al. (2007) Structures of the Cd44-hyaluronan complex provide insight into a fundamental carbohydrate-protein interaction. *Nat Struct Mol Biol* 14(3):234–239.
6. Jorgensen WL, Chandrasekhar J, Madura JD, Impey RW, Klein ML (1983) Comparison of simple potential functions for simulating liquid water. *J Chem Phys* 79:926–935.
7. Humphrey W, Dalke A, Schulten K (1996) VMD: visual molecular dynamics. *J Mol Graph* 14(1):33–38, 27–28.

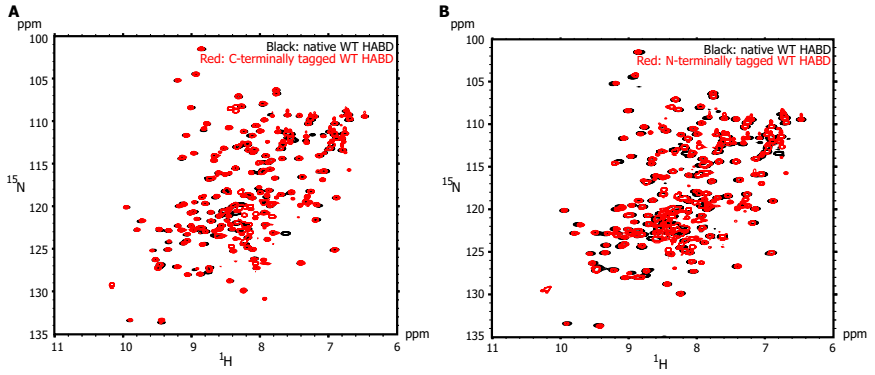

Fig. S1. NMR analysis of biotin-tagged HABDs. (*A*) Overlaid ^{1}H-^{15}N HSQC spectra of HABD with (red) and without (black) the C-terminal AviTag. (*B*) Overlaid ^{1}H-^{15}N HSQC spectra of HABD with (red) and without (black) the N-terminal AviTag.

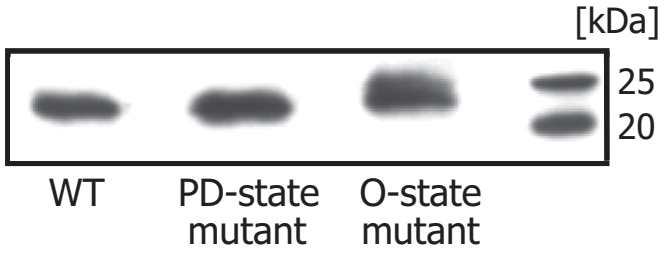

Fig. S2. Western blot analysis of the HABD-coated beads. The amounts of HABD (WT and O- and PD-state mutants) immobilized on microbeads were assessed by a Western blot analysis, using the anti-biotin mAb.

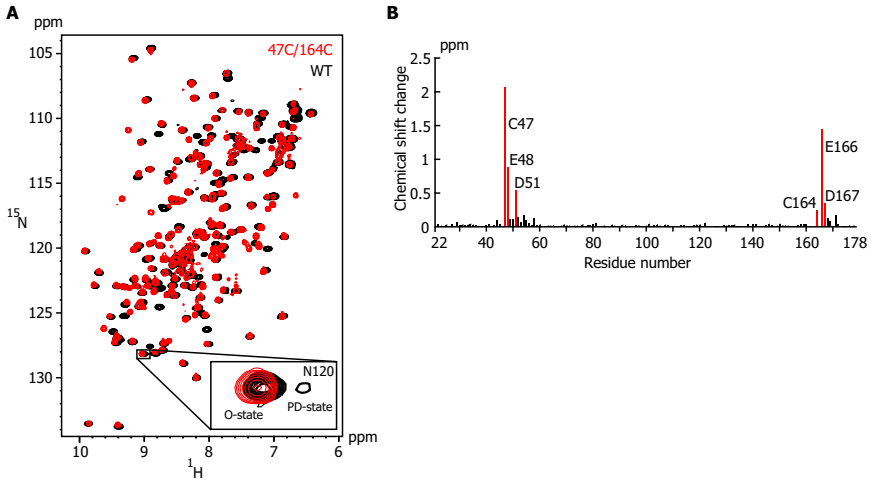

Fig. S3. NMR analysis of the O-state mutant. (*A*) Overlaid ^{1}H-^{15}N HSQC spectrum of the O-state mutant (T47C/N164C, red) and WT (black) HABD in the HA-free state. *Inset* shows signals derived from N120. (*B*) Chemical shift difference between the O-state mutant and WT. The weighted averages of the chemical shift differences were calculated with the function $\delta\Delta = [\{(\delta\Delta_{NH})^2 + (\delta\Delta_N/6.5)^2\}]^{1/2}$.

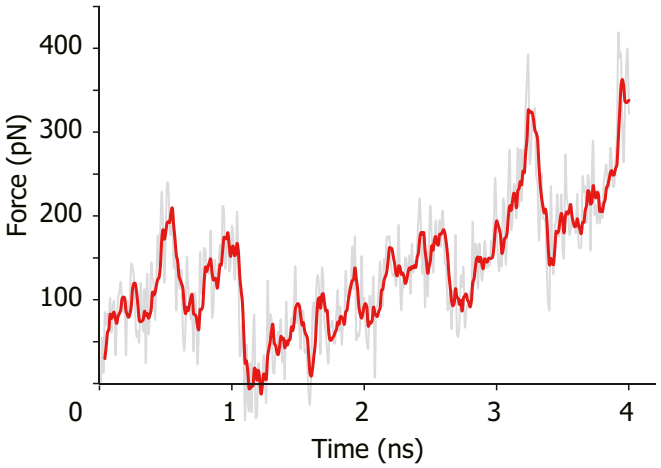

Fig. S4. Time series of the applied force from SMD simulations. Raw data are indicated in gray and 50-ps running average is indicated in red.

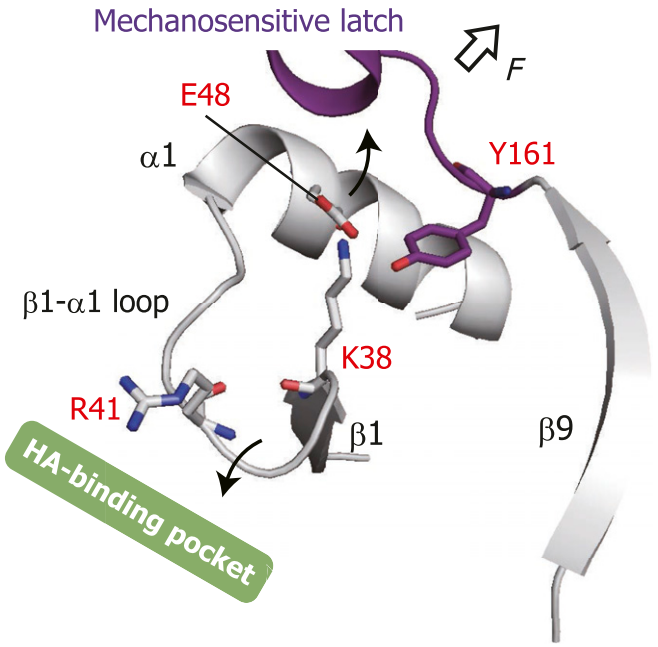

Fig. S5. Allosteric propagation from the mechanosensitive latch to the distal HA-binding site. The region engaging allosteric propagation is shown. The key conformational changes are shown by arrows.

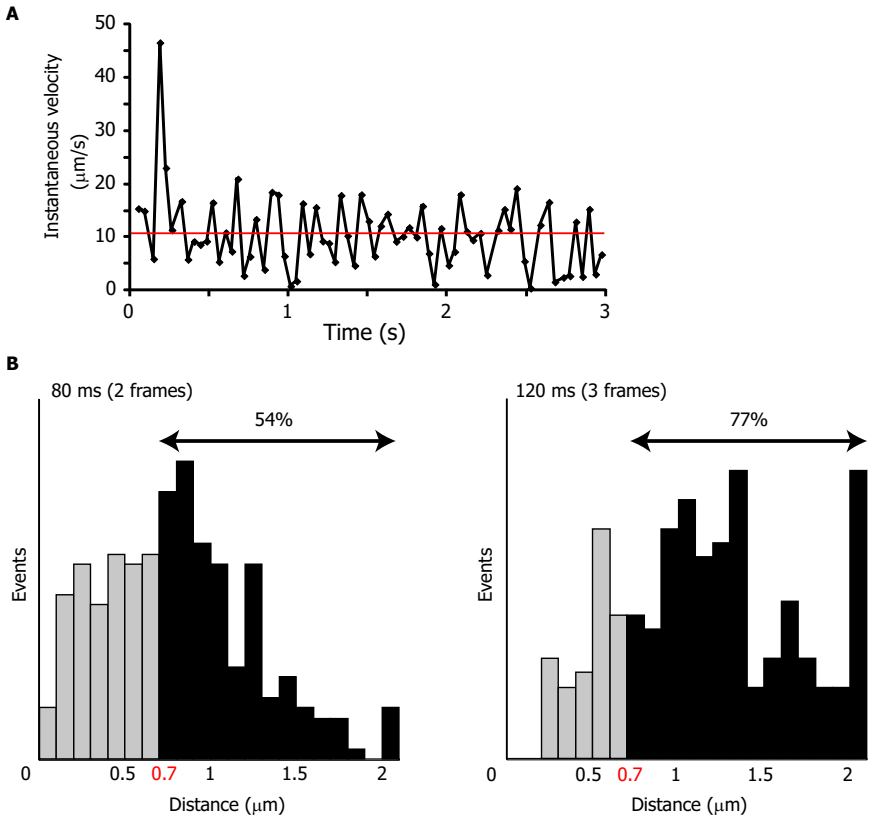

Fig. S6. Particle-tracking analysis of a bead rolling on the HA substrate. (*A*) Plot of the instantaneous velocity of a bead rolling on the HA substrate at 1.0 dyn/cm^2. The instantaneous velocity was calculated by measuring the displacement of the beads during a single frame (40 ms). The red line indicates the average velocity of the total event (10 μm/s). (*B*) Histograms of the distances over which beads moved during 80 ms (*Left*) and 120 ms (*Right*). Percentages of events where beads traveled more than 0.7 μm are indicated.

Table S1. The HA-binding constants of C- and N-terminally AviTagged HABDs

Construct	K_D
N-terminal	17.2 ± 2.3 μM
C-terminal	18.2 ± 2.4 μM

The SPR experiments were performed using the HA 12mer and the AviTagged HABD as ligand and analyte, respectively. The dissociation constants (K_D) were obtained from the steady-state curve-fitting analysis.

Table S2. Rolling parameters of the cell-free rolling experiment

Parameter	Value
Bead radius	5 μm
Fluid density	1 g/cm^3
HABD density	3,000–6,000/μm^2
HA density	0.2 pg/μm^2
Temperature	293 K
Reynolds no.*	0.5
Tether length	12 nm
Estimated tether angle	88.7°
Estimated total tether force†	3.4 nN·dyn^{-1}·cm^{-2}

*The Reynolds number was calculated as described previously (1).
†The total tether force was estimated by a force balance equation (2).

1. Bakker DP, van der Plaats A, Verkerke GJ, Busscher HJ, van der Mei HC (2003) Comparison of velocity profiles for different flow chamber designs used in studies of microbial adhesion to surfaces. *Appl Environ Microbiol* 69(10):6280–6287.
2. Alon R, Chen S, Puri KD, Finger EB, Springer TA (1997) The kinetics of L-selectin tethers and the mechanics of selectin-mediated rolling. *J Cell Biol* 138(5):1169–1180.